Journal of Applied Electrochemistry **32**: 641–646, 2002.

Porosity determination of nickel coatings on copper by anodic voltammetry

H.A. PONTE[1]* and A.M. MAUL[2]
[1]*Federal University at Paraná, Department of Chemical Engineer, Laboratory of Surface Electrochemistry and Corrosion (LESC), PO Box 19011, 81531-990, Curitiba, Paraná, Brazil*
[2]*Federal University at Paraná, Laboratory of Surface Electrochemistry and Corrosion (LESC), Curitiba, Paraná, Brazil*
*(*author for correspondence, e-mail: hponte@engquim.ufpr.br)*

Received 6 September 2001; accepted in revised form 26 March 2002

Key words: anodic voltammetry, electrochemical techniques, metallic coatings, porosity

Abstract

This paper presents the application of anodic voltammetry to determine the effective porosity in nickel coatings. The nickel coatings were obtained by electrodeposition from a Watts bath on copper substrate. This technique consists in a comparison of the charge density involved in the passivation process of the substrate without coating and that required to passivate the substrate covered with a nickel layer. The passivation solution was a 0.4 M sodium sulfide solution (Na_2SO_3) at 25 °C selected to maintain the coating inert in the potential region where substrate passivation occurs, thus preserving its integrity. The results indicate an exponential decay of the coating porosity, with respect to the deposit thickness, and a net porosity of 4 to 5%. The relation between porosity decay and deposition potential was investigated for nickel deposition from a Watts bath.

1. Introduction

Metallic coatings are frequently inspected visually to detect pores. However, a precise determination of the amount and distribution of the pores is required. Pores and cracks in metallic coatings are localized interruptions of the coating material that may be defined as follows: (a) *pores* are voids expanded predominantly in three dimensions, which are not filled with solid or liquid materials, and (b) *cracks* are faults with expansion predominantly in one dimension [1]. They can be classified as in Figure 1 [1], as (i) pores and cracks 'passer-bys' crossing the whole coating, from the surface to the substrate, and (ii) pores and cracks 'no-passer-bys', subdivided in opened 'no-passer-by' (opened to the surface but not reaching the substrate), and closed ones (no opening to the surface, totally restricted into the coating or substrate). In this work, pores and cracks of type 1 were studied. In general, the porosity in the electrodeposits is analysed qualitatively by four techniques: ferrocyanate test, electrographic test, hot water test and salt-spray test. These techniques are based on the observation and counting of pores, and, consequently, they are not sensitive to pores of small dimensions, which prevents the detection of small cracks, as well as small pores [2–5].

With the increasing interest in thin films technologies [6–8], there is a need for more reliable measuring techniques of coating porosity. Basically, the porosity measuring techniques can be divided into two categories: (i) techniques in which individual pores are detected by physical, chemical or electrochemical observation, and (ii) techniques in which the total porosity is obtained through measurements of gas permeation, chemical or electrochemical analysis [9]. Electrochemical measurement seem more appropriated to determines the effective coating porosity, including exposed substrate through pores and cracks of type 1. These techniques can be divided in four categories: open circuit potential measurements [10, 11], anodic current measurements [12–16], polarization resistance measurements [16], measurements of the charge obtained during process of potentiodynamic anodic polarization [10, 17] and, recently, cyclic voltammetric charge measurements [8].

This work presents the results obtained from voltammetric anodic dissolution, in which the dissolution/passivation charges of the substrate were measured. One positive aspect of this technique is the short analysis time (about one minute), when compared with current works [9]. In addition, the charges involved in the porosity analysis by the proposed technique are about 100 times smaller than those necessary to determine the porosity by other techniques [9]. As a consequence, a smaller interference level on the sample could be obtained, as well as a larger reliability and better precision [8]. Meanwhile, it should be noted that the applied technique uses a small area for analysis not considering possible edge effects.

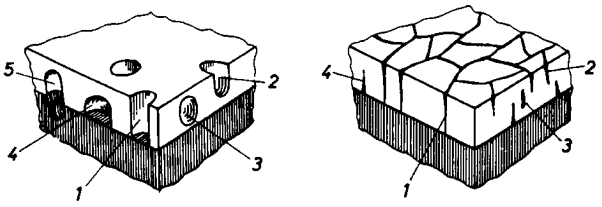

Fig. 1. Representation of the different types of pores and cracks. Type 1: pore/crack passer-by; type 2: open pore/crack, no-passer-by; type 3: closed pore/crack, restricted entirely in the coating; types 4 and 5: closed, contiguous and penetrating in the substrate, respectively [1]. (Reprinted with permission of the author).

2. Experimental procedures

The voltammetric anodic dissolution technique used in this work, consists of anodic polarization of the substrate/coating system and the measurement of the charge density involved in the passivation process of the substrate [18].

The comparison between the passivation charge densities of the substrate without coating (passivation standard charge density) and that involved in the passivation of the covered substrate, gives the porosity according to the expression [19, 20]:

$$\theta = \frac{Q_{\mathrm{PASS}}}{Q^{\circ}_{\mathrm{PASS}}} \tag{1}$$

where θ is the porosity or substrate area fraction exposed to electrolyte; $Q^{\circ}_{\mathrm{PASS}}$ is the dissolution/passivation charge for substrate without any coating; and Q_{PASS} is the covered substrate dissolution/passivation charge.

The necessary conditions to apply this technique are: the substrate does not suffer chemical attack in the dissolution/passivation solution, the substrate passivates and the coating must stay inert or present a small reaction rate in the potential range for passivation [21–24]. Due to the restrictions imposed by the above conditions and for the case of small reaction rates, between the dissolution/passivation solution and the coating, Equation 1 should be modified to:

$$\theta_i = \frac{Q_{\mathrm{PASS}} - (1-\theta_{i-1})Q_{\mathrm{REV}}}{Q^{\circ}_{\mathrm{PASS}}} \tag{2}$$

with: θ_i the porosity at the ith iteration; θ_{i-1} the porosity in the previous iteration; and Q_{REV} the coating dissolution/passivation charge.

From Equation 2, the porosity calculation is proposed as an iterative procedure, with the porosity obtained in the first iteration used for porosity calculation in the second iteration and so forth. In the first iteration $\theta_{i-1} = 0.5$ is used as a first estimative for the iterative process. Independent of the assumed value, along the iterations the porosity value tends to the correct value. The convergence condition used was that the variation between the last two iterations should be smaller than 1%.

In this work a nickel coating on copper was selected. Copper and nickel 99.9% purity grade electrodes were used to define the initial conditions. The nickel electrodeposition was carried out potentiostatically from a Watts bath with no organic additives consisting of 0.9 M nickel sulfate ($NiSO_4 \cdot 6H_2O$), 0.5 M boric acid (H_3BO_3), 0.2 M nickel chloride ($NiCl_2 \cdot 6H_2O$) and 1 M sulfuric acid (H_2SO_4) added to maintain pH at 3.5. The electrolyte used for the anodic voltammetry was a 0.4 M sodium

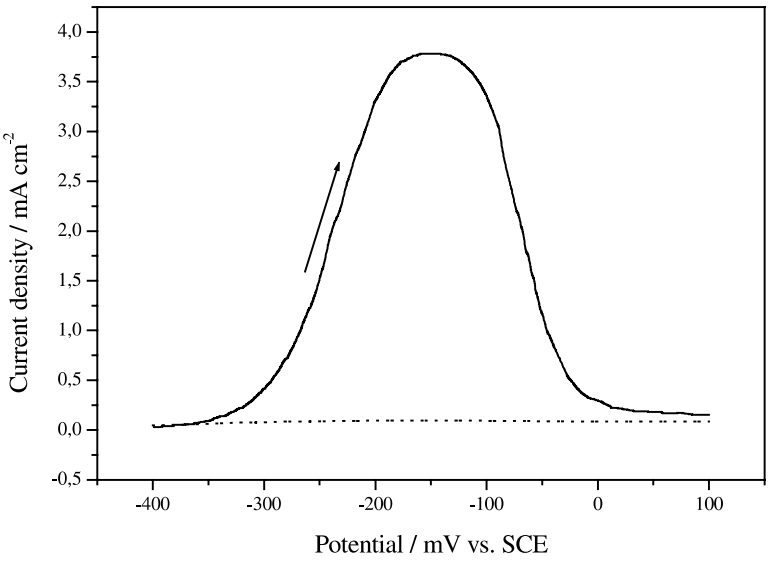

Fig. 2. Dissolution/passivation process of copper (—) and nickel (- - -) electrodes in a sodium sulfide electrolyte (Na_2SO_3) 0.4 M, scan rate 10 mV s^{-1}.

sulfide solution (Na_2SO_3) with pH = 10. All solutions were prepared from distilled water (conductivity 2.4 μS cm^{-1}) and analytical grade chemicals. They were maintained and used at room temperature (25 °C).

The copper working electrodes consisted of 18 disc electrodes, manufactured from a copper cylinder and individually assembled in small Teflon™ skirts. The exposed area of these electrodes was 0.119 cm^2. The electrodes were polished on emerypaper (brown aluminum oxide, Al_2O_3) to a 600 grit finish before use. All potentials were referred to the saturated calomel electrode (SCE). The nickel electrode was manufactured from a small nickel cylinder embedded in epoxy resin, type Araldite™, in a Pyrex™ glass tube. The exposed area was 0.226 cm^2. The counter electrode was a spiral platinum wire (dia. 1 mm).

For the anodic voltammetry, a potentiostat/galvanostat PAR model 273, coupled with a recorder was used. The surface morphology was analyzed by scanning electron microscopy (SEM) using a Phillps XL 30 microscope.

3. Results and discussion

Figure 2 presents a voltammetric analysis of copper and nickel for the anodic voltammetric polarization measurements at 0.4 M Na_2SO_3 solution. The copper passivation/dissolution process occurs in the range from −400 mV to 100 mV. In this potential range the nickel dissolution/passivation charge is small and can be quantified. Therefore, the three necessary conditions for the application of voltammetric anodic dissolution (VAD) in porosity analysis were fulfilled and the copper fraction exposed through nickel pores can be calculated using Equation 2.

Afterwards, a copper standard passivation charge density, Q°_{PASS}, can be determined, being the charge density involved in the clean copper passivation. The copper standard passivation charge density value, calculated from the area under the copper dissolution/passivation reaction curve presented in Figure 2, was 70.59 mC cm^{-2} for a polarization rate of 10 mV s^{-1}. It could also be observed that the nickel standard passivation charge density, Q_{REV}, determined for a nickel electrode was 4.2 mC cm^{-2}. The dissolution/passivation charge for the coating was obtained using a pure nickel electrode and the same polarization conditions as for the substrate. Nickel deposits were made on copper substrates at three deposition potentials (−850 mV, −930 mV, −1030 mV) and different deposition charge density Q_{DEP}. For each of these deposits, the copper dissolution/passivation charge, Q_{PASS}, was determined. The coating porosity was calculated from Equation 2. The deposition charge densities used in the deposition process ranged from 40 to 670 mC cm^{-2}, corresponding to thickness ranging from 0.014 to 0.230 μm. The surface damage after the application of the proposed technique was verified by scanning electron microscopy (SEM) (Figure 3). Scratches and small holes from sanding were observed (Figure 3(a)). Figure 3(b) presents a typical micrograph of the copper electrode covered with nickel after the dissolution/passivation process. Figure 3(c) shows a greater magnification of Figure 3(b). The deposition potential used was −1030 mV and the deposited nickel charge density was of 670 mC cm^{-2}. It is observed that the nickel deposit reproduced the copper morphology, with rugosity and amplification of superficial defects. This probably hap-

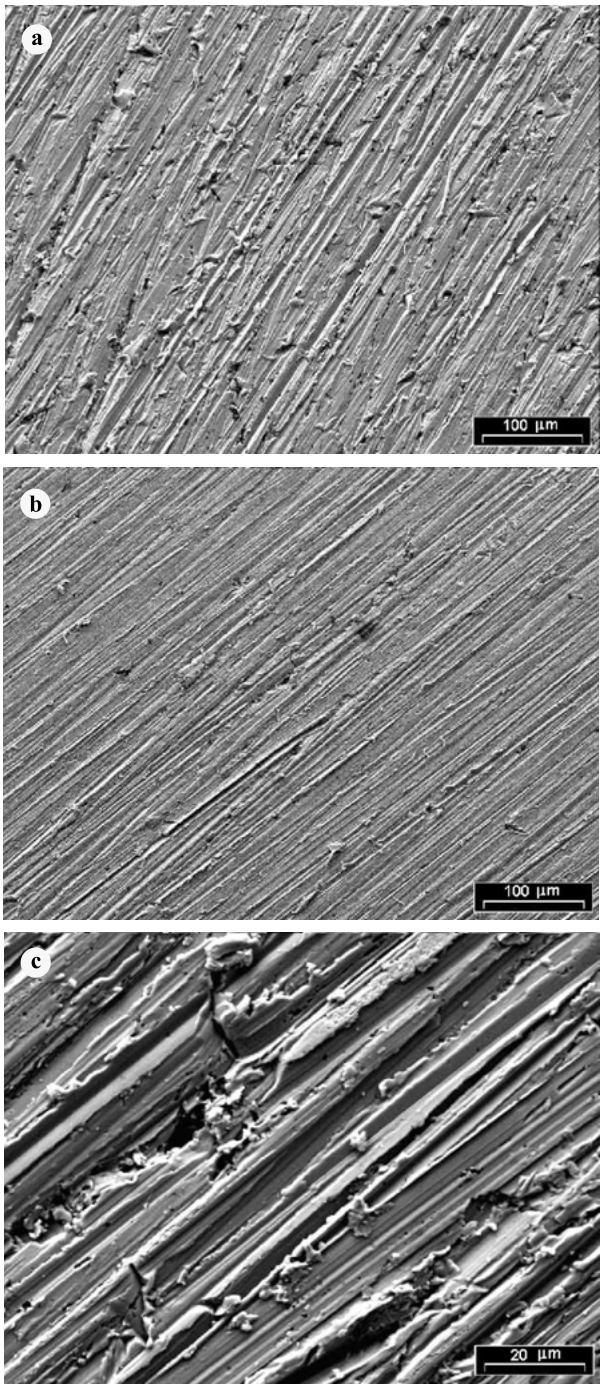

Fig. 3. (a) Copper electrode, (b) copper electrode coated by nickel after dissolution/passivation process, general view, and (c) detail of the center of the electrode. Conditions: deposition potential −1030 mV and deposited nickel charge density 670 mC cm^{-2}.

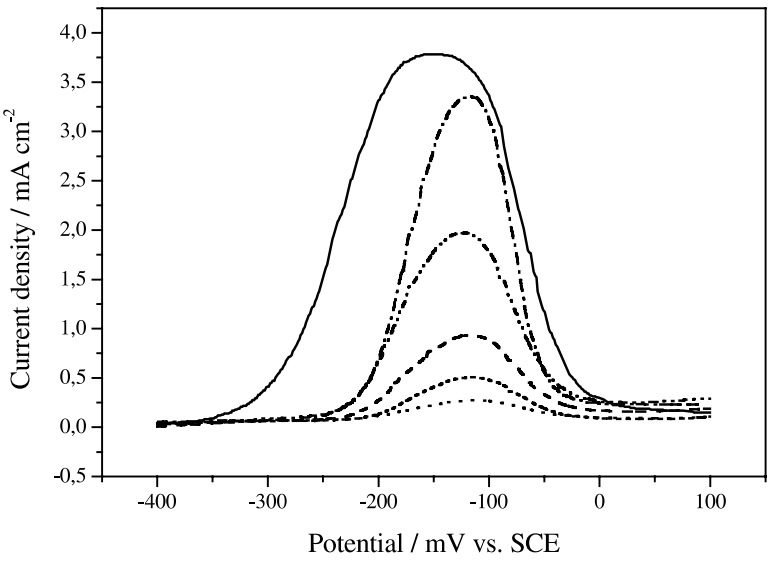

Fig. 4. Copper passivation curves for several nickel deposition charge densities. Conditions: deposition potential −830 mV, scan rate 10 mV s^{-1}. Charge: (—) standard; (– · – ·) 5, (– · · – · ·) 15, (– – –) 25, (· · · ·) 35 and (- - -) 50 mC.

pened due to the absence of organic additives, (i.e., levelling agents). The analytical processes seem to cause no damage to the coating.

In Figure 4, dissolution/passivation curves are presented for the deposition potential of −830 mV. As the nickel deposition charge increases, the dissolution/passivation charge decreases, indicating a decrease in the copper area exposed to the electrolyte. A shift of the initial potential for the copper passivation process is also evident. This shift occurs in the direction of more cathodic values from −350 mV for the pure copper, to −240 mV, when there is a nickel deposit on copper.

Figures 5 and 6 present the dissolution/passivation curves for the deposition potentials of −930 and −1030 mV. Characteristic porosity curves obtained using Equation 2, for the deposition potential of −830, −930 and −1030 mV, are presented in Figure 7. These curves were obtained by plotting the deposition charge density (mC cm^{-2}) against the porosity fraction obtained in the fourth iteration (θ_4).

The three exponential equations relating the porosity index, θ, to the deposition charge density, Q_{DEP} in mC cm^{-2}, obtained are as follows:
For deposition potential = −830 mV

$$\theta = \exp\left(\frac{-Q_{DEP}}{141.1}\right) \tag{3}$$

Thicknesses tested range from 0.014 to 0.144 μm.
For deposition potential = −930 mV

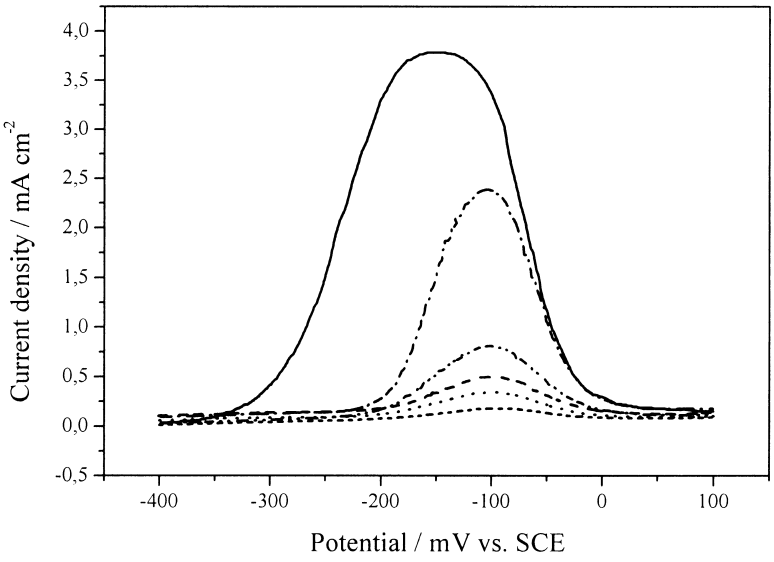

Fig. 5. Copper passivation curves for several nickel deposition charge densities. Conditions: deposition potential −930 mV, scan rate 10 mV s^{-1}. Charge: (—) standard; (– · – ·) 5, (– · · – · ·) 15, (– – –) 25, (· · · ·) 35 and (- - -) 50 mC.

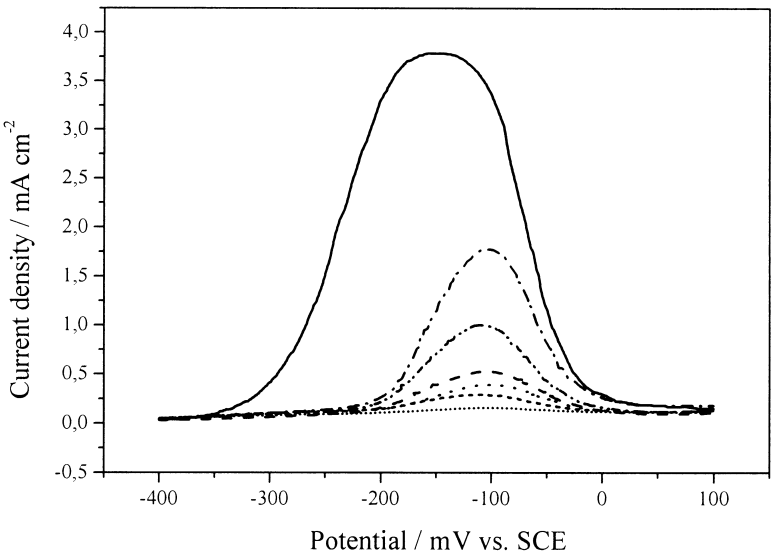

Fig. 6. Copper passivation curves for several nickel deposition charge densities. Conditions: deposition potential −1030 mV, scan rate 10 mV s^{-1}. Charge: (—) standard; (– · – · ·) 5, (– · · – · ·) 15, (– – –) 25, (· · · ·) 35, (- - -) 50 and (·····) 80 mC.

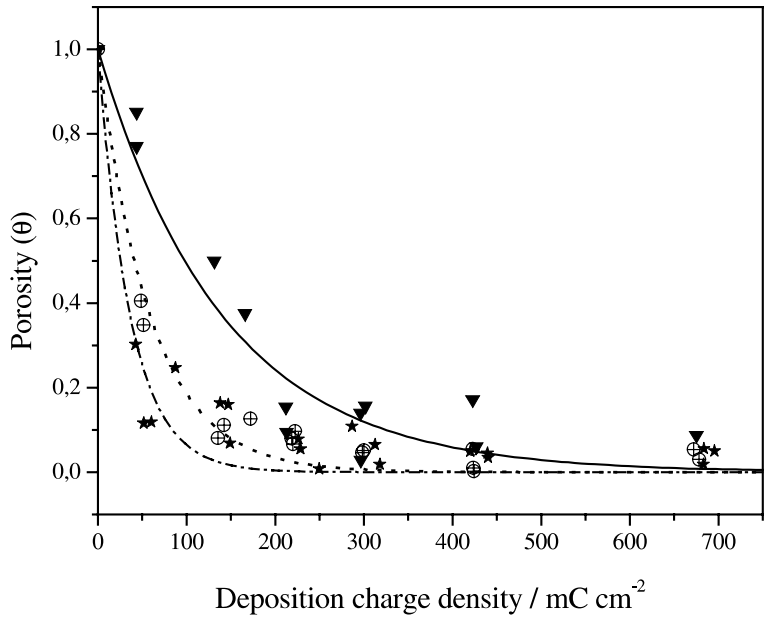

Fig. 7. Curves of nickel deposition charge density against porosity. Deposition potential: (▼) − 830, (⊕) − 930 and (★) − 1030 mV.

$$\theta = \exp\left(\frac{-Q_{DEP}}{59.3}\right) \quad (4)$$

Thicknesses tested range from 0.014 to 0.144 μm.
For deposition potential = −1030 mV

$$\theta = \exp\left(\frac{-Q_{DEP}}{36.4}\right) \quad (5)$$

Thicknesses tested range from 0.014 to 0.230 μm.

It can be seen that for the same deposition charge density, the coating obtained for more cathodic potentials, has smaller porosity. This smaller porosity may be associated with the larger deposition current density applied in the deposition process, leading to a higher nucleation rate and a consequent larger number of fine grains [17, 24]. High deposition overpotential results in finer grains [24, 25], but, for current densities higher than limiting, due to mass transport effects, the porosity tends to increase again [24].

It can also be observed that the porosity calculated based on the experimental data (Equations 3, 4 and 5) tends to zero ($\theta = 0.1\%$) for deposition charge densities in the order of 950, 450 and 250 mC cm^{-2}, for deposition potentials of −830, −930 and −1030 mV, respectively. In spite of this, for deposition charge densities in the order of 670 mC cm^{-2}, a residual passivation charge

density was observed indicating some residual porosity of about 4 to 5%. This residual porosity may be related to cracks produced by stress present in all the electrodeposited nickel process.

4. Conclusions

The voltammetric anodic dissolution (VAD) technique used for coating porosity measurements presented good sensitivity allowing a precise porosity evaluation. It was also possible to verify that deposits obtained at larger current densities have smaller porosity.

The technique developed can be applied for mechanically ground substrates (600 grit finishing) with no need of a better prepared surface.

The substrate composition allows the passivation process just during the polarization procedure, with no passive film formation before the anodic polarization. This electrochemical behaviour needs to be confirmed for other substrate compositions.

Acknowledgements

The authors are grateful to CAPES for the supported scholarship and to LACTEC for the SEM analysis.

References

1. T.W. Jelinek and K. Beyer, 'Prüfung von funktionellen metallischen Schichten', Vol. 26 (Leuzeverlag, Saulgau-Württ, Germany, (1997), pp. 127–129.
2. M. Aroyo and Zl. Parisheva, *Trans. Inst. Met. Finish.* **70** (1992) 168.
3. I.M. Notter and D.R. Gabe, *Trans. Inst. Met. Finish.* **68** (1990) 59.
4. P. Leisner and M.E. Benzon, *Trans. Inst. Met. Finish.* **75** (1997) 88.
5. E. Julve, Pint. Acabados Ind. (1986) 80.
6. W. Tato and D. Landolt, *J. Electrochem. Soc.* **145** (1998) 4173.
7. I. Yu Konyashin and T.V. Chukalowskaya, *Surf. Coat. Technol.* **88** (1996) 5.
8. M. Lakatos-Varsanyi and D. Hanzel, *Corros. Sci.* **41** (1999) 1585.
9. J.R. Roos, J.P. Celis and Fan Chonglun, *J. Electrochem. Soc.* **137** (1990) 1096.
10. T.P. Hoar, *J. Electrodepositors' Tech. Soc.* **14** (1938) 33.
11. R.J. Morrissey, *J. Electrochem. Soc.* **117** (1970) 742.
12. U.R. Evans and S.C. Shome, *J. Electrodepositors' Tech. Soc.* **26** (1950) 137.
13. U.R. Evans and S.C. Shome, *J. Electrodepositors' Tech. Soc.* **27** (1951) 45.
14. U.R. Evans and S.C. Shome, *J. Electrodepositors' Tech. Soc.* **27** (1951) 65.
15. W.O. Freitag, *J. Electrochem. Soc.* **117** (1970) 1239.
16. M. Clarke and A.M. Chakrabarty, *Trans. Inst. Met. Finish.* **48** (1970) 99.
17. J.P. Celis, J.R. Roos and C. Fan, *Trans. Inst. Met. Finish.* **69** (1991) 15.
18. A.M. Maul, MSc thesis, UFPR, PIPE (2001).
19. J.P. Celis, D. Drees, E. Maesen and J.R. Roos, *Thin Solid Films* **224** (1993) 58.
20. M. Lakatos-Varsanyi and Darko Hanzel, *Corros. Sci.* **41** (1999) 1585.
21. I.A. Carlos, DSc thesis, USP-IFQSCar, DQFM (1990).
22. H.A. Ponte, DSc thesis, UFSCar, DEMA (1994).
23. H.A. Ponte and A.M. Maul, *in* Anais do Interfinish Latino Americano – EBRATS 97, ABTS, São Paulo, SP (1997).
24. C. Fan, J.P. Celis and J.R. Roos, *J. Electrochem. Soc.* **138** (1991) 2917.
25. M. Clarke and A.M. Chakrabarty, *Trans. Inst. Metal. Finish.* **48** (1970) 99.